ADBA
Intelligent Systems for Chemical and Materials Science
Cutting-Edge Scientific Solutions

e-ISSN:3150-0021
RESEARCH ARTICLE
Vol.1 / No.1 / 2026
pp. 26-34 / Article No. e005
https://doi.org/10.69882/adba.iscms.2026075

Computational Investigation of Sn Addition Effects on Phase Stability and Transformation Kinetics in Zr-Sn-Cr Alloys

Halil Can Gedik *,1 **and Özgür Özdilli** *,2

*Department of Mechanical Engineering, Faculty of Engineering and Natural Sciences, Hitit University, Çorum, Türkiye

ABSTRACT This study presents a computational investigation into the effects of tin (Sn) content variation on the phase stability, phase transformation behavior, and transformation kinetics of Zr-Sn-Cr ternary alloys. Using the JMatPro thermokinetic simulation software, phase fraction diagrams and time-temperature-transformation (TTT) diagrams were constructed for three alloy compositions: Zr-0.1Cr-1.5Sn, Zr-0.1Cr-3.0Sn, and Zr-0.1Cr-6.0Sn (all in wt.%), with chromium content held constant at 0.1 wt.%. The results demonstrate that increasing Sn content significantly enhances the stability and formation temperature of the Zr_4Sn intermetallic phase while concurrently reducing the alpha phase fraction. The C15_FCC ($ZrCr_2$) Laves phase exhibited minimal sensitivity to Sn addition in terms of phase fraction, though its onset formation temperature increased progressively. Furthermore, Sn enrichment was found to elevate the alpha-beta transformation temperatures while narrowing the beta phase stability range, indicating reduced beta phase stability. TTT diagram analysis revealed accelerated alpha phase precipitation kinetics with increasing Sn content, as evidenced by shorter precipitation times and higher formation temperatures. These findings provide valuable insights for the design of Sn-containing zirconium alloys for nuclear cladding and other high-temperature applications.

KEYWORDS
Zirconium alloys
Zr-Sn-Cr system
JMatPro
Phase diagrams
TTT diagrams
Zr_4Sn
Phase stability
Computational thermodynamics

INTRODUCTION

Zirconium-based alloys have garnered significant attention in the nuclear industry due to their exceptional corrosion resistance, low thermal neutron absorption cross-section, and favorable mechanical properties at elevated temperatures (Liu *et al.* 2025). Among the various alloying elements employed in Zr alloy design, tin (Sn) plays a pivotal role as a strengthening agent and stabilizer of the alpha phase in Zircaloy-type alloys. The addition of Sn to Zr alloys has been shown to influence phase equilibria, precipitation behavior, and transformation kinetics, all of which are critical factors in determining the in-service performance of nuclear fuel cladding materials (Jerlerud Pérez *et al.* 2008; Subasic 1998).

The Zr-Sn binary system has been extensively studied, with the Zr_4Sn intermetallic phase identified as a key precipitate formed via the peritectoid reaction $\beta Zr + Zr_5Sn_3 \leftrightarrow Zr_4Sn$ at approximately 1598 ± 20 K (Russell and Lee 2005; Northwood and Lim 1979). Recent studies have also established that Sn addition affects the alpha-beta transformation temperatures, with Sn reportedly increasing the $\alpha + \beta \leftrightarrow \beta$ transformation temperature while decreasing the $\alpha \leftrightarrow \alpha + \beta$ temperature (Popov and Proselkov 2005; Canay *et al.* 2000). However, the influence of Sn on ternary Zr-Sn-Cr systems, particularly regarding the competitive phase stability between Zr_4Sn, alpha-Zr, and C15 Laves phases, remains insufficiently characterized.

The emergence of computational materials science has enabled systematic investigation of alloy phase equilibria and transformation kinetics through Calphad-based thermodynamic databases and kinetic simulation tools. JMatPro (Java-based Materials Properties) has proven to be a powerful platform for calculating phase diagrams, thermophysical properties, and transformation kinetics of multi-component alloys (Saunders *et al.* 2003). This approach has been successfully applied to investigate the compositional effects on thermodynamic properties and phase stability in various alloy systems. For instance, computational studies employing

Manuscript received: 24 May 2026,
Revised: 28 June 2026,
Accepted: 19 July 2026,
Published: 30 August 2026.

[2]ozgurozdilli@hitit.edu.tr (**Corresponding author**).

JMatPro have investigated the effect of aluminum content on the thermodynamic properties and phase stability of Mg-Al-Zn alloys, demonstrating the efficacy of computational modeling in predicting phase evolution (Uzunoğlu 2025a). Similarly, the same methodology has been utilized to examine the influence of aluminum and vanadium content variation on the thermodynamic properties of Ti-Al-V alloys, establishing a robust framework for computational alloy design (Uzunoğlu 2025b).

The present study adopts the same computational approach to systematically investigate the effects of Sn content variation on phase formation, phase stability, and transformation kinetics in the Zr-Sn-Cr system. Specifically, three compositions—Zr-0.1Cr-1.5Sn, Zr-0.1Cr-3.0Sn, and Zr-0.1Cr-6.0Sn (wt.%)—were modeled using JMatPro to construct phase fraction diagrams as a function of temperature and time-temperature-transformation (TTT) diagrams. The chromium content was maintained constant at 0.1 wt.% to isolate the effect of Sn variation. The calculated phase diagrams and TTT diagrams provide a comprehensive understanding of how Sn enrichment alters phase equilibria and precipitation kinetics, offering guidance for the compositional optimization of Zr-based alloys for nuclear and high-temperature applications.

METHODOLOGY

Computational Approach

All thermodynamic and kinetic calculations were performed using JMatPro (version 9.1), a computational materials engineering software that integrates thermodynamic databases with physical property models to simulate the behavior of multi-component alloys (Saunders *et al.* 2003; Garner *et al.* 2015). The Zr alloy module of JMatPro incorporates thermodynamic data for elements including Zr, Cr, Fe, Hf, Nb, Ni, Si, Sn, C, H, N, and O, enabling comprehensive phase equilibrium calculations for Zr-based systems (Liu *et al.* 2025). The software calculates phase equilibria by minimizing the Gibbs free energy of the system and provides outputs including phase fractions as a function of temperature, phase transformation temperatures, and TTT/CCT diagrams.

Alloy Compositions

In this study, three alloy compositions were investigated by systematically varying the tin content while keeping the chromium content constant at 0.1% by weight. The designed alloy compositions are shown in Table 1.

Phase Fraction Diagram Calculations

Equilibrium phase fraction diagrams were calculated for each composition over a temperature range of 200°C to 2000°C. The calculations considered the following phases: alpha-Zr (hcp solid solution), beta-Zr (bcc solid solution), Zr_4Sn (tetragonal intermetallic), C15_FCC ($ZrCr_2$ Laves phase, cubic), and liquid. The phase fractions were determined as a function of temperature under equilibrium conditions.

TTT Diagram Calculations

Time-temperature-transformation (TTT) diagrams were constructed for each alloy composition to evaluate the precipitation kinetics of alpha phase during isothermal holding. The calculations were performed with an assumed ASTM grain size of 4.5, and the transformation start temperatures for alpha grain boundary (GB) and alpha matrix precipitation were determined at 0.5% transformation fraction. The TTT diagrams provide critical information on the incubation times and temperature ranges for alpha phase formation, which are essential for understanding the hardenability and heat treatment response of these alloys.

RESULTS AND DISCUSSION

Proposed Model Overview

Figure 1 presents the schematic overview of the computational modeling approach employed in this study. The model integrates thermodynamic calculations of phase diagrams with kinetic simulations of TTT diagrams to provide a comprehensive understanding of how Sn content variation affects phase stability and transformation behavior in Zr-Sn-Cr alloys. This integrated approach, which combines equilibrium thermodynamics with non-equilibrium transformation kinetics, has been validated in previous computational studies on Mg-Al-Zn and Ti-Al-V alloy systems (Uzunoğlu 2025a,b). The model enables systematic prediction of phase fractions, transformation temperatures, and precipitation kinetics as a function of alloy composition, providing a rational basis for alloy design and optimization.

Phase Fraction Diagrams

Zr-0.1Cr-1.5Sn Alloy Figure 2 shows the equilibrium phase fraction diagram for the Zr-0.1Cr-1.5Sn (wt.%) alloy as a function of temperature. The diagram reveals several distinct phase regions:

- **Alpha phase (α-Zr):** Stable from room temperature up to approximately 895°C, with a maximum fraction of approximately 98% at lower temperatures. The alpha phase fraction gradually decreases with increasing temperature as the alloy approaches the alpha-beta transformation region.
- **Beta phase (β-Zr):** Begins to form at approximately 895°C, with its fraction increasing progressively until the alloy becomes fully beta at approximately 1750°C. The beta phase exhibits maximum stability in the high-temperature regime.
- **Zr_4Sn phase:** This intermetallic phase appears at approximately 459°C and remains stable down to room temperature. The Zr_4Sn fraction reaches a maximum of approximately 5-6% in the intermediate temperature range.
- **C15_FCC phase ($ZrCr_2$):** The C15 Laves phase forms at approximately 688°C and exhibits a relatively small fraction (<1%) throughout its stability range.
- **Liquid phase:** Appears at approximately 1750°C and increases with temperature until complete melting occurs at approximately 1833°C.

The formation of Zr_4Sn via the peritectoid reaction $\beta Zr + Zr_5Sn_3 \leftrightarrow Zr_4Sn$ at approximately 1598 K (1325°C) is consistent with previously reported experimental data (Russell and Lee 2005; Northwood and Lim 1979). The presence of the C15_FCC phase, corresponding to the cubic $ZrCr_2$ Laves phase, is in agreement with the established Zr-Cr phase diagram, where C15 is the stable low-temperature polymorph of $ZrCr_2$ below approximately 1846 K (1573°C).

Zr-0.1Cr-3.0Sn Alloy Figure 3 presents the phase fraction diagram for the Zr-0.1Cr-3.0Sn (wt.%) alloy. The increased Sn content from 1.5% to 3.0% produces several notable changes in phase equilibria:

- **Alpha phase stability:** The maximum alpha phase fraction decreases from approximately 98% to approximately 95%, reflecting the reduced Zr content available for alpha solid solution formation. The alpha → alpha+beta transformation temperature increases from approximately 883°C to approximately 921°C.

Table 1 Three alloy compositions designed for modeling in JMatPro

Alloy Designation	Zr (wt.%)	Cr (wt.%)	Sn (wt.%)
Zr-0.1Cr-1.5Sn	98.4	0.1	1.5
Zr-0.1Cr-3.0Sn	96.9	0.1	3.0
Zr-0.1Cr-6.0Sn	93.9	0.1	6.0

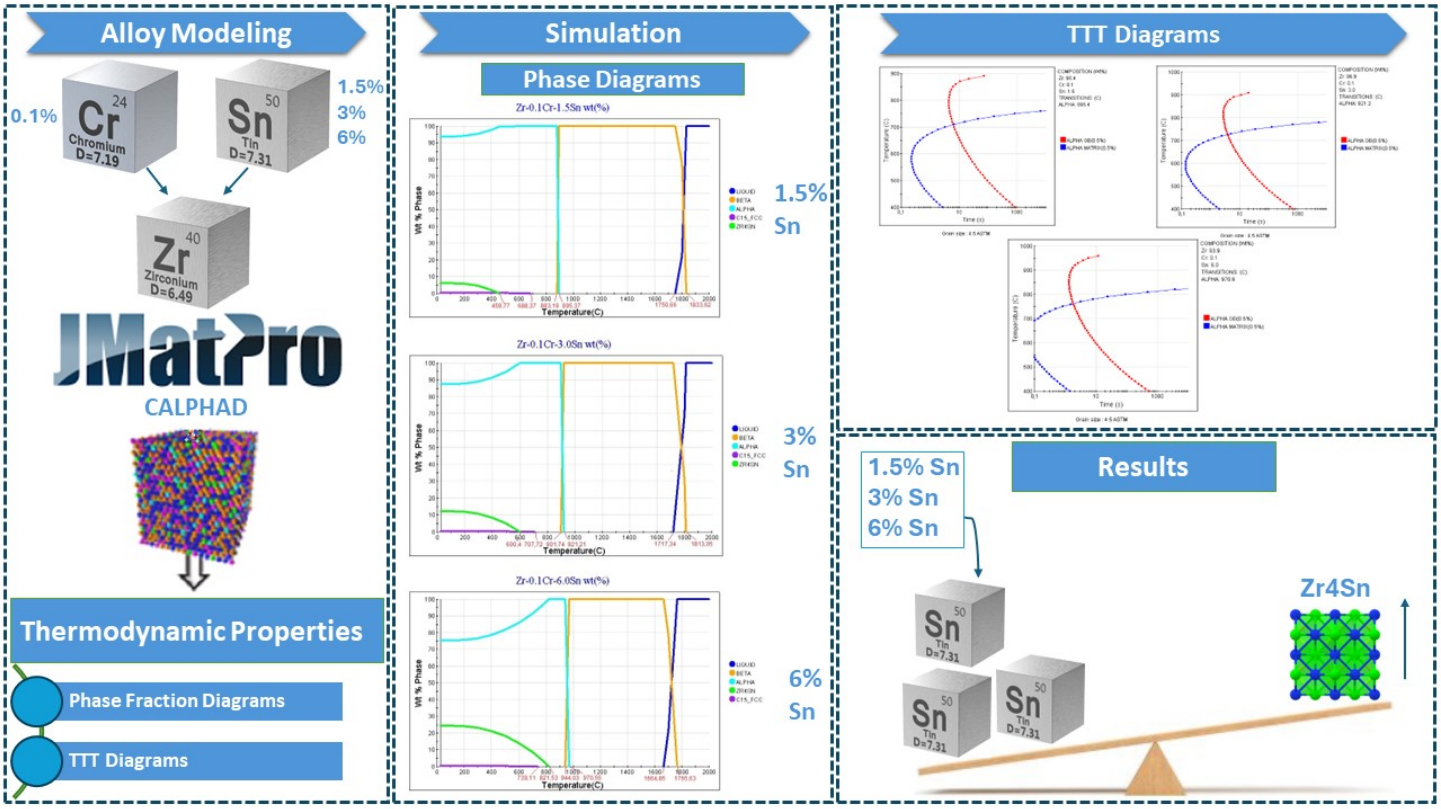


Figure 1 Proposed model schematic illustrating the integrated computational approach combining phase diagram calculations and TTT diagram simulations for Zr-Sn-Cr alloy systems.

- **Zr_4Sn phase:** The Zr_4Sn phase fraction increases significantly compared to the 1.5% Sn alloy, reaching approximately 10-12% in the intermediate temperature range. The onset temperature for Zr_4Sn formation increases from 459°C to approximately 600°C.
- **C15_FCC phase:** The C15 phase fraction remains relatively unchanged (∼1%), but its formation temperature increases from 688°C to approximately 707°C.
- **Beta phase:** The beta phase stability range narrows, with the beta start temperature decreasing from approximately 883°C to approximately 901°C. The beta → liquid transformation temperature decreases from approximately 1833°C to approximately 1813°C.
- **Liquidus temperature:** The liquidus temperature decreases from approximately 1750°C to approximately 1717°C, indicating that Sn addition lowers the melting point of the alloy.

Zr-0.1Cr-6.0Sn Alloy Figure 4 displays the phase fraction diagram for the Zr-0.1Cr-6.0Sn (wt.%) alloy, representing the highest Sn content investigated. The most pronounced changes are observed at this composition:

- **Alpha phase:** The alpha phase fraction is further reduced to approximately 85-90%, with the alpha → alpha+beta transformation temperature increasing to approximately 970°C. As the stability of the Zr_4Sn phase increases, the stability range of the alpha phase narrows significantly.
- **Zr_4Sn phase:** The Zr_4Sn phase fraction reaches its maximum among the three compositions, approaching approximately 20-25% in the intermediate temperature range. The onset temperature for Zr_4Sn formation increases to approximately 821°C, demonstrating a clear trend of enhanced Zr_4Sn stability with increasing Sn content.
- **C15_FCC phase:** The C15 phase fraction remains at approximately 1%, with the formation temperature increasing to approximately 739°C. This suggests that while Sn addition does not significantly affect the amount of C15 phase formed, it does influence the temperature at which this phase becomes thermodynamically stable.

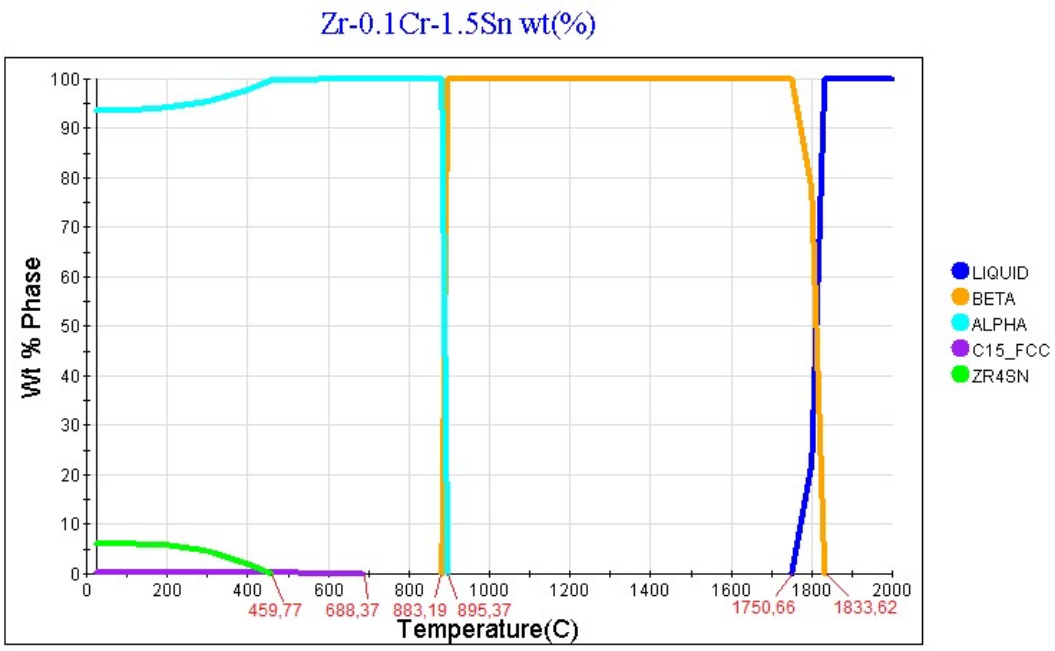


Figure 2 Equilibrium phase fraction diagram for Zr-0.1Cr-1.5Sn (wt.%) alloy as a function of temperature.

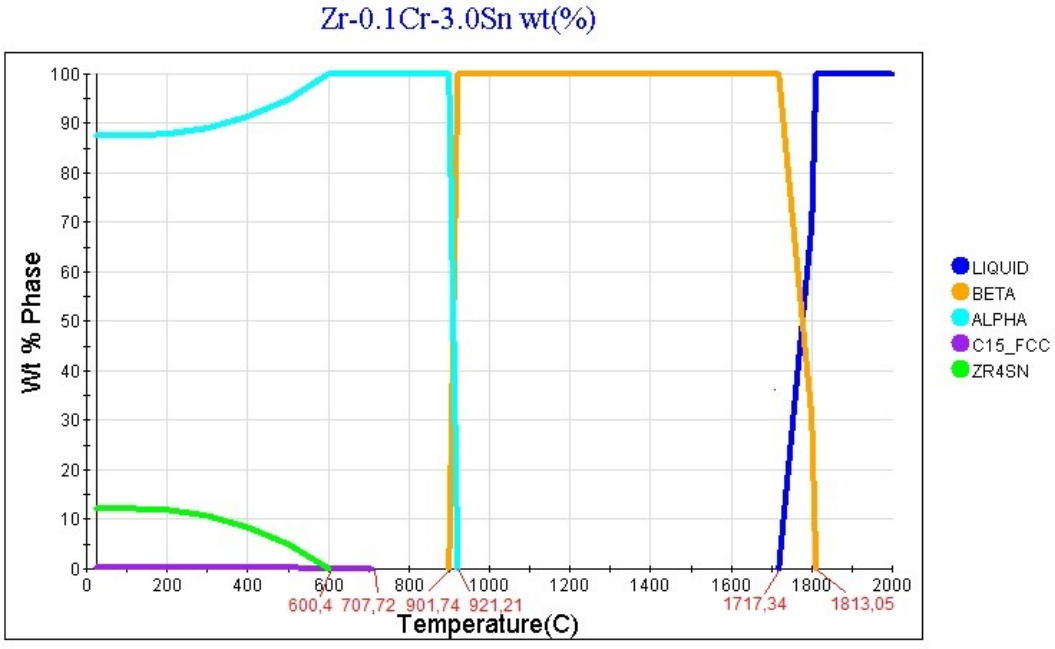


Figure 3 Equilibrium phase fraction diagram for Zr-0.1Cr-3.0Sn (wt.%) alloy as a function of temperature.

- **Beta phase:** The beta phase stability range continues to narrow, with the beta start temperature decreasing to approximately 944°C. The beta → liquid transformation temperature decreases further to approximately 970°C.
- **Liquidus temperature:** The liquidus temperature decreases to approximately 1664°C, confirming the trend of reduced melting temperatures with increasing Sn content.

Effect of Sn Content on Phase Stability

Zr_4Sn Phase Stability The results from the phase fraction diagrams demonstrate a clear and systematic effect of Sn content on Zr_4Sn phase stability. As summarized in Table 1, increasing the Sn content from 1.5 wt.% to 6.0 wt.% results in:

The increased stability of Zr_4Sn with higher Sn content is consistent with thermodynamic expectations, as the phase requires Sn for its formation through the peritectoid reaction. The observed

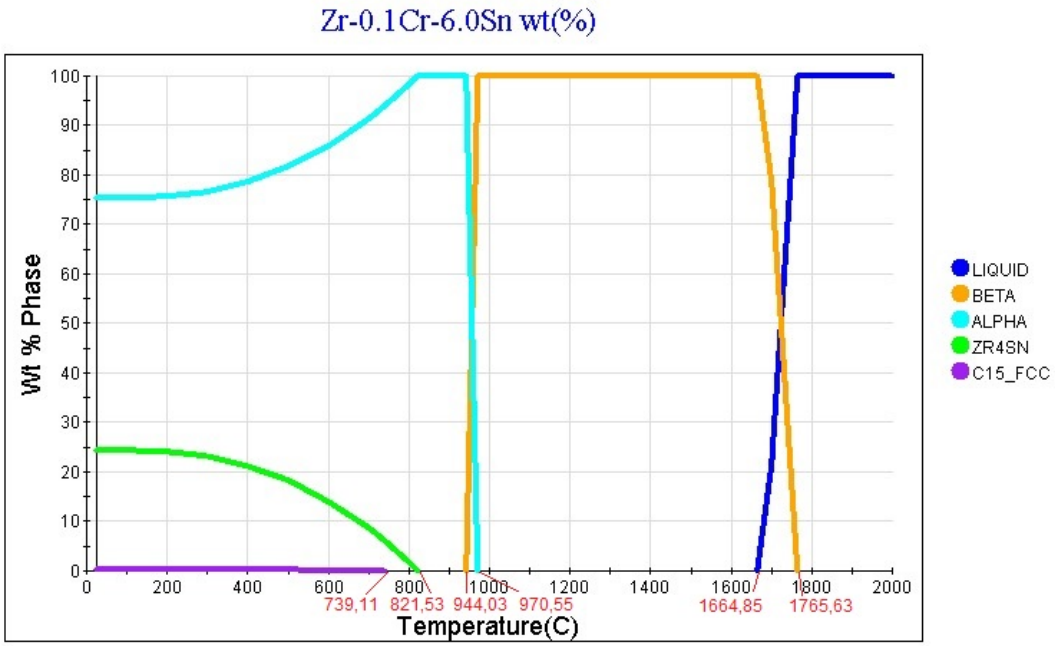


Figure 4 Equilibrium phase fraction diagram for Zr-0.1Cr-6.0Sn (wt.%) alloy as a function of temperature.

Table 1 Summary of key phase transformation temperatures and phase fractions as a function of Sn content in Zr-0.1Cr-xSn alloys.

Property	Zr-0.1Cr-1.5Sn	Zr-0.1Cr-3.0Sn	Zr-0.1Cr-6.0Sn
Zr_4Sn onset temperature (°C)	459.77	600.4	821.53
Maximum Zr_4Sn fraction (%)	∼5-6	∼10-12	∼20-25
Alpha → alpha+beta temperature (°C)	895	921	970
Beta start temperature (°C)	∼883	∼901	∼944
Beta → liquid temperature (°C)	1833.62	1813.05	1765.63

increase in Zr_4Sn formation temperature from 688°C to 739°C indicates that Sn enrichment shifts the peritectoid reaction to higher temperatures, expanding the stability field of this intermetallic phase. This finding aligns with previous experimental observations that the Zr_4Sn phase is stable at temperatures between 800-1050°C and that its decomposition is influenced by the presence of interstitial elements such as oxygen (Jerlerud Pérez *et al.* 2008; Cui *et al.* 2024; Kwon and Corbett 1992). Oxygen modifies the thermodynamic stability of the Zr_4Sn intermetallic phase, thereby influencing its formation and decomposition behavior (Kwon and Corbett 1992).

The increased Zr_4Sn fraction at higher Sn contents necessarily reduces the alpha phase fraction, as both phases compete for the available Zr atoms. This competition is evident in the phase diagrams, where the alpha phase fraction decreases systematically as Sn content increases. The trade-off between Zr_4Sn precipitation and alpha solid solution formation has important implications for the mechanical properties and corrosion resistance of these alloys, as Zr_4Sn precipitates can serve as strengthening particles but may also deplete the matrix of Sn, affecting the solid solution strengthening effect.

C15_FCC Phase Stability The C15_FCC ($ZrCr_2$) Laves phase exhibits a different response to Sn addition compared to the Zr_4Sn phase. While the C15 phase fraction remains relatively constant at approximately 1% across all three compositions, its formation temperature increases from 688°C to 739°C with increasing Sn content. This suggests that Sn does not significantly affect the thermodynamic stability of the C15 phase in terms of phase fraction, but it does influence the temperature at which this phase becomes thermodynamically favorable.

The C15 $ZrCr_2$ phase is known to be the stable low-temperature polymorph of the $ZrCr_2$ Laves phases, with the C14 phase being stable at high temperatures and the C36 phase serving as an intermediate polymorph. The observed formation temperatures for the C15 phase (688-739°C) are well below the C15 → C36 transformation temperature of approximately 1846 K (1573°C), consistent with the established phase stability of $ZrCr_2$. The slight increase in C15 formation temperature with Sn addition may be attributed

to the influence of Sn on the chemical potentials of Zr and Cr in the ternary system, as suggested by experimental thermodynamic investigations of the Cr-Nb-Sn-Zr system, which demonstrated the complex phase equilibria involving Zr-, Cr-, and Sn-containing intermetallic compounds (Lafaye *et al.* 2019).

Alpha-Beta Transformation Behavior The alpha-beta transformation behavior is significantly affected by Sn content. The results show that; alpha $\rightarrow$ alpha+beta transformation temperature increases from approximately 895°C (1.5% Sn) to 970°C (6.0% Sn). This indicates that Sn acts as an alpha stabilizer, raising the temperature at which the alpha phase begins to transform to beta. Beta start temperature decreases from approximately 883°C (1.5% Sn) to 944°C (6.0% Sn). The beta phase becomes stable over a narrower temperature range as Sn content increases. Beta $\rightarrow$ liquid transformation temperature decreases from 1833°C to 1765°C, reflecting the melting point depression effect of Sn addition.

These observations are consistent with literature reports on the effect of Sn on phase transformation temperatures in Zr alloys. Studies have shown that Sn increases the $\alpha + \beta \leftrightarrow \beta$ transformation temperature while decreasing the $\alpha \leftrightarrow \alpha + \beta$ temperature. The present results confirm that this trend holds in the ternary Zr-Sn-Cr system, with the overall effect being a narrowing of the beta phase stability field.

The narrowing of the beta phase stability range with increasing Sn content has important implications for the thermomechanical processing of these alloys. A narrower beta phase field means that the alloy must be processed within a more restricted temperature window to achieve the desired beta-phase microstructure. This could affect the hot working and heat treatment schedules required to optimize the mechanical properties of Sn-containing Zr alloys.

Time-Temperature-Transformation (TTT) Diagrams

Zr-0.1Cr-1.5Sn Alloy Figure 5 presents the TTT diagram for the Zr-0.1Cr-1.5Sn alloy, showing the isothermal transformation behavior of alpha phase. The diagram exhibits the characteristic C-curve shape, with the following key features:

- **Alpha transformation start temperature:** The alpha phase begins to form at approximately 895°C, which corresponds to the alpha $\rightarrow$ beta transformation temperature identified in the phase fraction diagram.
- **Alpha grain boundary (GB) precipitation:** At 0.5% transformation fraction, alpha grain boundary precipitation occurs over a temperature range of approximately 600-850°C, with the minimum incubation time (nose of the C-curve) occurring at approximately 700-750°C.
- **Alpha matrix precipitation:** Matrix precipitation of alpha phase occurs at slightly lower temperatures and longer times compared to grain boundary precipitation, reflecting the higher activation energy required for nucleation within the grain interior.
- **Precipitation kinetics:** At the nose temperature ($\sim$700°C), the time required for 0.5% alpha transformation is approximately 10-100 seconds, indicating relatively rapid precipitation kinetics.

Zr-0.1Cr-3.0Sn Alloy Figure 6 shows the TTT diagram for the Zr-0.1Cr-3.0Sn alloy. The increased Sn content produces significant changes in the transformation kinetics:

- **Alpha transformation start temperature:** Increases to approximately 900°C, consistent with the elevated alpha $\rightarrow$ beta transformation temperature observed in the phase diagram.
- **Nose temperature:** The nose of the C-curve shifts to higher temperatures (approximately 750-800°C) compared to the 1.5% Sn alloy.
- **Precipitation kinetics:** The incubation times for alpha precipitation are significantly reduced. At the nose temperature, the time required for 0.5% transformation decreases to approximately 1-10 seconds, indicating accelerated precipitation kinetics.
- **Temperature range:** The overall temperature range for alpha precipitation narrows, with the transformation occurring over a more restricted temperature interval.

Zr-0.1Cr-6.0Sn Alloy Figure 7 presents the TTT diagram for the Zr-0.1Cr-6.0Sn alloy, representing the highest Sn content:

- **Alpha transformation start temperature:** Further increases to approximately 970°C, reflecting the continued elevation of the alpha $\rightarrow$ beta transformation temperature with Sn addition.
- **Nose temperature:** The nose of the C-curve shifts to even higher temperatures (approximately 800-850°C).
- **Precipitation kinetics:** The incubation times continue to decrease, with 0.5% transformation occurring in less than 1 second at the nose temperature. This indicates extremely rapid precipitation kinetics.
- **Temperature range:** The transformation temperature range is further narrowed, consistent with the reduced beta phase stability field observed in the phase diagram.

Effect of Sn on Transformation Kinetics The TTT diagram results reveal a systematic effect of Sn content on alpha phase precipitation kinetics:

- **Accelerated precipitation:** Increasing Sn content significantly reduces the incubation time for alpha phase precipitation. This is attributed to the increased driving force for alpha formation resulting from the elevated alpha $\rightarrow$ beta transformation temperature and the reduced beta phase stability.
- **Elevated nose temperature:** The nose of the C-curve shifts to higher temperatures with increasing Sn content, indicating that the maximum precipitation rate occurs at higher temperatures.
- **Narrowed transformation window:** The temperature range over which alpha precipitation occurs becomes narrower with increasing Sn content, reflecting the reduced beta phase stability field.

These kinetic effects are consistent with the thermodynamic changes observed in the phase fraction diagrams. The increased driving force for alpha formation (resulting from the elevated alpha $\rightarrow$ beta transformation temperature) accelerates the precipitation kinetics, while the reduced beta phase stability narrows the temperature window for transformation.

The accelerated alpha precipitation kinetics with Sn addition has important implications for the heat treatment and processing of these alloys. Faster precipitation means that the alloy will be more susceptible to alpha phase formation during cooling from the beta phase field, potentially affecting the final microstructure and mechanical properties. The shift of the nose temperature to higher temperatures also means that the alloy will be more sensitive to transformations during cooling through the high-temperature range.

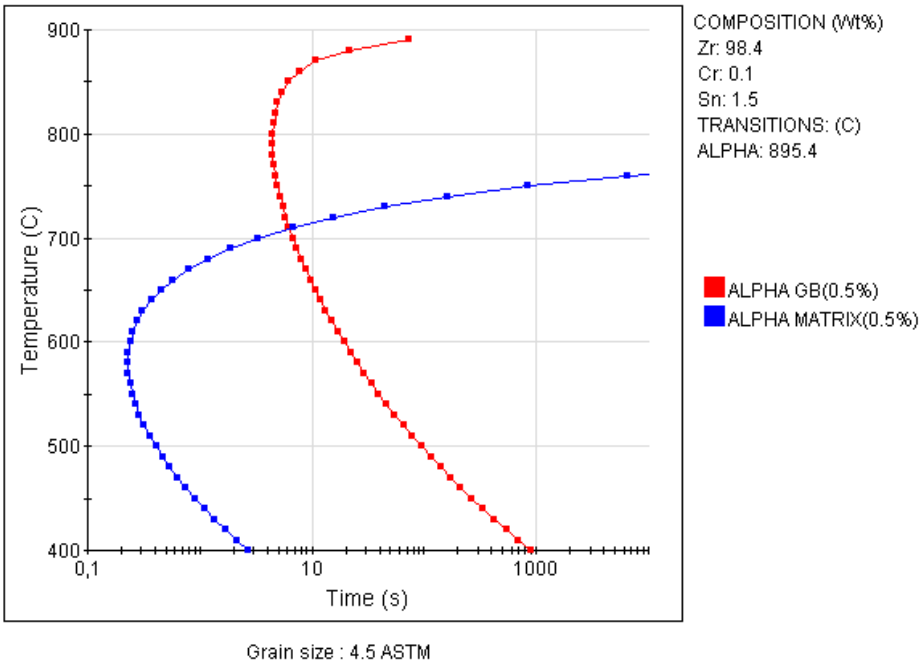


Figure 5 Time-temperature-transformation (TTT) diagram for Zr-0.1Cr-1.5Sn (wt.%) alloy showing alpha grain boundary (GB) and alpha matrix precipitation at 0.5% transformation fraction.

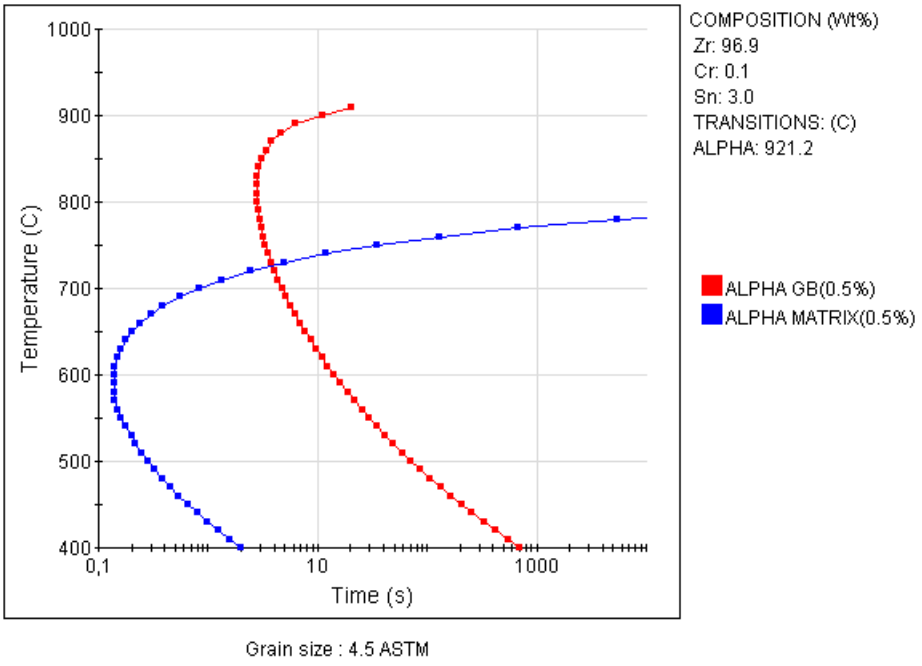


Figure 6 Time-temperature-transformation (TTT) diagram for Zr-0.1Cr-3.0Sn (wt.%) alloy showing alpha grain boundary (GB) and alpha matrix precipitation at 0.5% transformation fraction.

Integration of Phase Diagram and TTT Diagram Results

The phase fraction diagrams and TTT diagrams provide complementary information on the phase stability and transformation behavior of Zr-Sn-Cr alloys. The key relationships between these two sets of results are:

- **Thermodynamic driving force:** The phase fraction diagrams establish the equilibrium phase stability and transformation temperatures, which define the thermodynamic driving force for phase transformations. The TTT diagrams then reveal the kinetics of these transformations under non-equilibrium conditions. The observation that increasing Sn content elevates the alpha → beta transformation temperature (phase diagram) and accelerates alpha precipitation (TTT diagram) is consistent with the increased thermodynamic driving force for alpha formation.

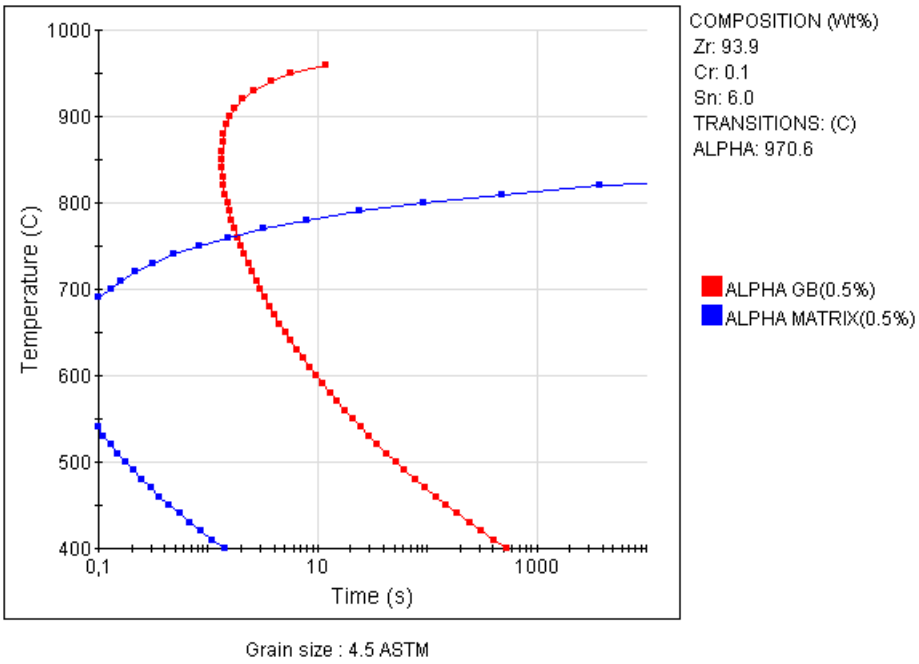


Figure 7 Time-temperature-transformation (TTT) diagram for Zr-0.1Cr-6.0Sn (wt.%) alloy showing alpha grain boundary (GB) and alpha matrix precipitation at 0.5% transformation fraction.

- **Temperature dependence:** The phase fraction diagrams show that the alpha phase is stable at lower temperatures and transforms to beta at higher temperatures. The TTT diagrams show that alpha precipitation occurs most rapidly at intermediate temperatures (the nose of the C-curve), where the driving force for transformation is balanced by diffusional mobility. The shift of the nose temperature to higher values with Sn addition (TTT diagram) correlates with the elevation of the alpha-beta transformation temperature (phase diagram).
- **Compositional effects:** Both sets of diagrams demonstrate that Sn content has a systematic effect on phase behavior. The phase diagrams show that Sn increases Zr_4Sn stability and decreases alpha phase fraction, while the TTT diagrams show that Sn accelerates alpha precipitation kinetics. These effects are thermodynamically consistent, as the increased Zr_4Sn formation reduces the Sn content available in the matrix, potentially affecting the kinetics of alpha formation.
- **Beta phase stability:** The phase diagrams reveal that Sn addition narrows the beta phase stability field, while the TTT diagrams show that alpha precipitation occurs over a narrower temperature range. This consistency confirms that Sn acts to destabilize the beta phase relative to alpha, promoting the alpha $\rightarrow$ beta transformation at higher temperatures.

The integration of thermodynamic and kinetic information provided by this combined approach enables a comprehensive understanding of the phase behavior of Zr-Sn-Cr alloys. This understanding is essential for the rational design of alloy compositions and processing conditions to achieve desired microstructures and properties.

CONCLUSIONS

This computational study of Zr-Sn-Cr alloys with varying Sn content (1.5, 3.0, and 6.0 wt.%) and constant Cr content (0.1 wt.%) has revealed several important findings regarding phase stability and transformation kinetics:

- **Zr_4Sn phase stability:** Increasing Sn content significantly enhances the stability and fraction of the Zr_4Sn intermetallic phase. The onset temperature for Zr_4Sn formation increases from 688°C to 739°C, and the maximum phase fraction increases from approximately 2-3% to 10-12% as Sn content increases from 1.5% to 6.0%. This is attributed to the increased availability of Sn for the peritectoid reaction $\beta Zr + Zr_5Sn_3 \leftrightarrow Zr_4Sn$.
- **Alpha phase behavior:** The alpha phase fraction decreases systematically with increasing Sn content, reflecting the competition between alpha solid solution and Zr_4Sn precipitation for available Zr atoms. The alpha $\rightarrow$ alpha+beta transformation temperature increases from 688°C to 739°C, indicating that Sn acts as an alpha stabilizer.
- **C15_FCC phase:** The C15 ($ZrCr_2$) Laves phase fraction remains relatively constant ($\sim$1%) across all compositions, though its formation temperature increases from 688°C to 739°C with Sn addition. This suggests that Sn does not significantly affect the thermodynamic stability of the C15 phase in terms of phase fraction, but does influence the temperature at which it forms.
- **Beta phase stability:** Increasing Sn content narrows the beta phase stability field, with the beta start temperature decreasing from $\sim$895°C to $\sim$821°C and the beta $\rightarrow$ liquid transformation temperature decreasing from 1833°C to 1765°C. This indicates that Sn destabilizes the beta phase relative to alpha.
- **Transformation kinetics:** TTT diagram analysis reveals that increasing Sn content accelerates alpha phase precipitation kinetics, as evidenced by shorter incubation times and elevated nose temperatures. The time required for 0.5% alpha transformation decreases from approximately 10-100 seconds to less than 1 second at the nose temperature as Sn content increases from 1.5% to 6.0%.
- **Integrated understanding:** The combined phase diagram and

TTT diagram analysis provides a comprehensive understanding of how Sn content affects both the thermodynamic driving forces and kinetic barriers for phase transformations in Zr-Sn-Cr alloys. This integrated approach enables the rational design of alloy compositions and processing conditions for optimized microstructures and properties.

The findings of this study contribute to the fundamental understanding of phase behavior in Sn-containing Zr alloys and provide a computational framework for the design of Zr-based alloys for nuclear cladding and other high-temperature applications.

Ethical Standard

The author have no relevant financial or non-financial interests to disclose.

Funding

This research received no external funding.

Data Availability Statement

The data supporting the findings of this study are available from the corresponding author upon reasonable request.

Conflict of Interest

The authors declares no conflict of interest.

LITERATURE CITED

Canay, M., C. A. Danón, and D. Arias, 2000 Phase transition temperature in the zr-rich corner of zr-nb-sn-fe alloys. Journal of Nuclear Materials **280**: 365–371.

Cui, J., P. Benigni, M. Barrachin, R. Ducher, G. Mikaelian, *et al.*, 2024 Revisiting the thermodynamic properties of the zrcr2 laves phases by combined approach using experimental and simulation methods. Journal of Alloys and Compounds **1002**: 175186.

Garner, A., J. Hu, A. Harte, P. Frankel, C. Grovenor, *et al.*, 2015 The effect of sn concentration on oxide texture and microstructure formation in zirconium alloys. Acta Materialia **99**: 259–272.

Jerlerud Pérez, R., C. Toffolon-Masclet, J.-M. Joubert, and B. Sundman, 2008 The zr–sn binary system: New experimental results and thermodynamic assessment. Calphad **32**: 593–601.

Kwon, Y. U. and J. D. Corbett, 1992 Influence of oxygen on the stability of zirconium-tin (zr4sn). Chemistry of Materials **4**: 187–190.

Lafaye, P., C. T. Masclet, J. C. Crivello, and J. M. Joubert, 2019 Experimental investigations and thermodynamic modelling of the cr–nb–sn–zr system. Calphad **64**: 43–54.

Liu, L. C., J. T. Zheng, Z. P. Wu, Z. Y. Xu, and S. F. Zhou, 2025 Effect of alloying elements on stacking fault energy and softening/hardening of zirconium. Journal of Materials Research and Technology **35**: 353–359.

Northwood, D. O. and D. T. Lim, 1979 Phase transformations in zirconium and its alloys. Canadian Metallurgical Quarterly **18**: 441–467.

Popov, S. G. and V. N. Proselkov, 2005 Heat capacity in two-phase regions and heat of phase transformations of certain zr-nb binary alloys. Atomic Energy pp. 451–463.

Russell, A. M. and K. L. Lee, 2005 *Structure-Property Relations in Nonferrous Metals - Chapter 12 Ti, Zr, and Hf*. Wiley-Interscience John Wiley & Sons, Inc.

Saunders, N., U. K. Z. Guo, X. Li, A. P. Miodownik, and J.-P. Schillé, 2003 Using jmatpro to model materials properties and behavior. JOM **55**: 60–65.

Subasic, N., 1998 Thermodynamic evaluation of sn-zr phase diagram. Calphad **22**: 157–165.

Uzunoğlu, Y., 2025a Computational study of the effect of aluminum content on the thermodynamic properties and phase stability of mg-al-zn alloys. ADBA Computer Science **2**: 36–42.

Uzunoğlu, Y., 2025b Effect of aluminum and vanadium content variation on the thermodynamic properties of ti–al–v alloys. Russian Metallurgy **2025**: 1760–1775.

How to cite this article: Gedik, H. C. and Özdilli, Ö. Computational Investigation of Sn Addition Effects on Phase Stability and Transformation Kinetics in Zr-Sn-Cr Alloys. *Intelligent Systems for Chemical and Materials Science*, 1(1), 26-34, 2026

Licensing Policy: The published articles in ISCMS are licensed under a Creative Commons Attribution-NonCommercial 4.0 International License.

